Asian Journal of
Science, Technology, Engineering, and Art

e-ISSN: 3025-4507
p-ISSN: 3025-5287

Index: Harvard, Boston, Sydney University, Dimensions, Lens, Scilit, Semantic, Google, etc

https://doi.org/10.58578/AJSTEA.v3i2.4941

Simulations and Modeling of Turbulence Flow Pattern in Pipe

A. A. Adetoyinbo[1], A. K. Bello[2], A. J. Omoliki[3]
[1,3]University of Ibadan, Nigeria; [2]Bells University of Technology, Ota, Nigeria
akbellokazeem@gmail.com; akbellokazeem@yahoo.com

Article Info:

Submitted:	Revised:	Accepted:	Published:
Jan 11, 2025	Jan 23, 2025	Feb 5, 2025	Feb 10, 2025

Abstract

This work is aimed at generating numerical simulations and modeling the turbulence flow pattern in pipes for water using Reynolds averaged Navier stokes equation. This is accomplished by using commercially available software called Cosmol Multiphysics in simulating and modeling the turbulence flow pattern of water in pipes at constant length but varying diameters of 0.16m, 0.15m, and 0.25m. The turbulence pattern was evaluated along the pipe by dividing the pipe into layers of 0.025m each. The turbulence pattern is found to be high in the middle of the pipe. The fluids at the boundary layer are found to have the same pattern for all the pipes.

Keywords: Time-Averaged, Turbulent Pipe Flows, Numerical Simulations, Modeling

Introduction

Fluid Dynamics is the branch of Physics that deals with fluids in motion. It is a study about liquid and gases flowing usually in and around solid surfaces. It can be quite a useful study that is used in several machines. Fluid Dynamics is further divided into two sections which are Aerodynamics, the study of the flow of air around aeroplanes and other automobiles so as to increase motion efficiency. Some of its principles are even used in traffic engineering, where traffic is treated as a continuous fluid (Acheson, 1990). The fact that the fluid is made up of discrete molecules is ignored (Batchelor, 1967). The Navier–Stokes equations are nonlinear partial in almost every real situation and linear equations for cases, such as one-dimensional flow and Stokes flow or creeping flow. The nonlinearity is due to convective acceleration, which is associated with the change in velocity over position. Hence, any convective flow, whether turbulent or not, will involve nonlinearity. Such flows can often be thoroughly studied and understood (Potter *et al,* 2008). According to some thought, the Navier–Stokes equations describe turbulence properly (Lerner *et al*., 1991). Another technique for solving numerically the Navier–Stokes equation is the large eddy simulation (LES), (Launder, 1991*).* According to (Scarslli *et al,* 2019) some developed methods are associated with the mechanical motion of the wall in certain channel cross-section or flow parameters impact in some cross-section and change in the flow structure or velocity profile. In other to suppress turbulence in pipes, there is need for special forming devices that approximately modify the profile of the average velocity at outlet (Lushchik, *et al,* 2023). There is flow relaminarization in pipes at Reynolds numbers $Re > 10000$ due to turbulence at the inlet and relaminarization occur up to Reynolds number Re = 16 000. Lushchik *et al.,* (2023). A device for formation of laminar submerged jets make it achievable to create smooth velocity profile with turbulent intensity than 1% for Reynolds number $Re > 10000$ at the initial jet diameter 0.12 m (Zaiko, *et al*., 2018 and Zayko *et al*., 2018). Flow in fluid can be laminar or turbulent. Laminar is the smooth and orderly flow of fluid particles in parallel layers of streams. The fluid moves in a predictable manner with minimal mixing between adjacent layers. It is commonly observed in situations where fluid velocity is high, the flow rate is low, and the conduit or channel through which the fluid flows has a smooth surface. (Encyclopedia Britannica). In fluid dynamics, laminar flow is a flow regime characterized by high momentum diffusion and low momentum convection (Geankpolis, 2003). For flow in a pipe of diameter D, experimental observations show that for "fully developed" flow, laminar flow occurs when the Reynold number is less than 2300. The common application of laminar flow would be in the smooth flow of a viscous liquid through a tube or pipe. In that case, the velocity of flow varies from zero at the walls to a maximum along the centerline of the vessel. Turbulent fluid motion can be define as an irregular condition of the flow in which various quantities show a random variation with time and space coordinates, so that statistically distinct average values can be discerned. Turbulence refers to the chaotic and irregular motion of fluid particles leading to mixing eddies, and fluctuations in velocity (Encyclopedia Britannica). It is believed, though not known with certainty, that the Navier–Stokes equations describe turbulence properly (Lesieur, 1990).

METHODS

The Reynolds Averaged Navier Stokes equation algebraic model known as the k-ϵ model is a very useful and common model for predicting turbulence. The commercial software used for this work is called Comsol 4.0 Multiphysics Software which uses the principle of finite element method to solve for the already averaged Navier Stokes equation.

Derivation of Reynolds Average Navier Stokes Equation

In a compressible Newtonian fluid, the Navier-Stokes equations read in absence of source terms in coordinate invariant formulation as

$$\frac{\partial \rho}{\partial t} + \frac{\partial}{\partial x_i}(\rho v_i) = 0 \tag{1a}$$

$$\frac{\partial}{\partial t}(\rho v_i) + \frac{\partial y}{\partial x}\left(\rho v_j v_i\right) = -\frac{\partial p}{\partial x_i} + \frac{\partial \tau_{ij}}{\partial x_j} \tag{1b}$$

$$\frac{\partial}{\partial t}(\rho E) + \frac{\partial y}{\partial x}\left(\rho v_j H\right) = -\frac{\partial}{\partial x_j}\left(v_i \tau_{ij}\right) + \frac{\partial}{\partial x_j}\left(K\frac{\partial T}{\partial x_j}\right) \tag{1c}$$

In above Equation (1a-c), $\boldsymbol{v_i}$ denotes a velocity component($\vec{v} = [v_1 v_2 v_3]^\tau$), stands for a coordinate direction, respectively. The components of the viscous stress tensor τ_{ij} are defined as

$$\tau_{ij} = 2\mu S_{ij} + \lambda \frac{\partial v_i}{\partial x_k}\delta_{ij} = 2\mu S_{ij} - \left(\frac{2\mu}{3}\right)\frac{\partial v_i}{\partial x_k}\delta_{ij} \tag{2}$$

The second term in equation 2 i.e. $\frac{\partial v_i}{\partial x_k}$, which corresponds to the divergence of velocity, disappear for incompressible flows in which this work was focused on. The components of the strain rate tensor are given by:

$$S_{ij} = \frac{1}{2}\left(\frac{\partial v_i}{\partial x_j} + \frac{\partial v_j}{\partial x_i}\right) \tag{3}$$

In this connection, let us also define the rotation rate tensor (antisymmetric part of the velocity gradient tensor) with the following components

$$\Omega_{ij} = \frac{1}{2}\left(\frac{\partial v_i}{\partial x_j} - \frac{\partial v_j}{\partial x_i}\right) \tag{4}$$

The total energy E and the total enthalpy H in equation 1c are obtained from the formulae:

$$E = e + \frac{1}{2}v_i v_i, \quad H = h + \frac{1}{2}v_i v_i \tag{5}$$

For incompressible flows we can reduce equations (1a-c) to the form:

$$\frac{\partial v_i}{\partial x_i} = 0 \tag{6a}$$

$$\frac{\partial v_i}{\partial t} + v_j\frac{\partial v_i}{\partial x_j} = -\frac{1}{\rho}\frac{\partial p}{\partial x_i} + \upsilon\nabla^2 v_i \tag{6b}$$

$$\frac{\partial T}{\partial t} + v_j\frac{\partial T}{\partial x_j} = k\nabla^2 T \tag{6c}$$

Where $\upsilon = {}^{\mu}/_{\rho}$ being the kinematic viscosity coefficient and ∇^2 denotes the Laplace operator.

Reynold Averaging

The first approach for the approximate treatment of turbulent flows was presented by Reynolds in 1895. The methodology is based on the decomposition of the flow variables into a mean and a fluctuating part. The governing equations (1a-c) are then solved for the mean values, which becomes the basis for turbulence model. Thus, considering first incompressible flows, the velocity components and the pressure in Eq. (1a-c) are substituted by

$$v_i = \bar{v}_i + v_i', p = \bar{p} + p' \tag{7}$$

The mean value is denoted by an over bar and the turbulent fluctuations by a prime. The mean values are obtained by an averaging procedure. There are three different forms of the Reynolds averaging, namely:

1. Time averaging - appropriate for stationary turbulence statistically steady turbulence
$$\bar{v}_{\mathrm{i}} = \lim_{\mathrm{T}\to\infty} \frac{1}{\mathrm{T}} \int_{\mathrm{t}}^{\mathrm{t+T}} v_{\mathrm{i}} \mathrm{dt} \tag{8}$$

As a consequence, the mean value ν_{i} does not vary in time, but only in space.

2. Spatial averaging - appropriate for homogeneous turbulence
$$\bar{v}_{\mathrm{i}} = \lim_{\Omega\to\infty} \frac{1}{\Omega} \int_{\Omega}^{\Omega+1} v_{\mathrm{i}} \mathrm{d}\Omega \tag{9}$$

Where Ω is the control volume. In this case, $\nu_{\mathrm{i}}$is uniform in space, but it is allowed to vary in time

3. Ensemble averaging - appropriate for general turbulence
$$\bar{v}_{\mathrm{i}} = \lim_{\mathrm{N}\to\infty} \frac{1}{\mathrm{N}} \sum_{\mathrm{m}=1}^{\mathrm{N}} v_{\mathrm{i}} \tag{10}$$

Here, the mean value $\bar{v}_{\mathrm{i}}$ still remains a function of time and of space coordinates.

Boussinesq Hypothesis

Many turbulence models are based upon the Boussinesq hypothesis. It was experimentally observed that turbulence decays unless there is shear in isothermal incompressible flows. Turbulence was found to increase as the mean rate of deformation increases. Boussinesq proposed in 1877 that the Reynolds stresses could be linked to the mean rate of deformation (Boussinesq, 1897).

Using the suffix notation where *i, j,* and *k* denote the *x, y,* and *z* directions respectively, viscous stresses are given by:

$$\tau_{\mathrm{ij}} = \mu \mathrm{S}_{\mathrm{ij}} = \mu \left(\frac{\partial v_{\mathrm{i}}}{\partial \mathrm{x}_{\mathrm{j}}} + \frac{\partial v_{\mathrm{j}}}{\partial \mathrm{x}_{\mathrm{i}}} \right) \tag{11}$$

He also proposed that the Reynolds stresses is similarly linked to the mean rate of deformation as shown in equation 11

$$T_{ij} = -\rho\overline{v_i' v_j'} = \mu_t\left(\frac{\partial v_i}{\partial x_j} + \frac{\partial v_j}{\partial x_i}\right) \tag{12}$$

Where μ_t is turbulent viscosity and it is also known as Eddy viscosity.

If we apply either the time averaging or the ensemble averaging to the Incompressible Navier-Stokes equations, we obtain the following relations for the mass and momentum conservation

$$\frac{\partial v_i}{\partial x_i} = 0 \tag{13a}$$

$$\rho\frac{\partial \bar{v}_i}{\partial t} + \rho\bar{v}_j\frac{\partial \bar{v}_i}{\partial x_j} = -\frac{\partial p}{\partial x_i} + \frac{\partial}{\partial x_j}\left(\bar{\tau}_{ij} - \rho\overline{v_i' v_j'}\right) \tag{13b}$$

These are known as the Reynolds-Averaged Navier-Stokes equations (RANS). The equations (5) are formally identical to the Navier-Stokes equations (1) or (2) with the exception of the additional term

$$T_{ij} = -\rho\overline{v_i' v_j'} = -\rho\left(\overline{v_i' v_j'} - \bar{v}_i\bar{v}_j\right) \tag{14}$$

T_{ij} is called Reynolds-stress tensor. It represents the transfer of momentum due to turbulent fluctuations. The fundamental problem of turbulence modeling based on the Reynolds-averaged Navier-Stokes equations is to find six additional relations in order to close the equations.

K-ϵ Two-Equation Model

The K-ε turbulence model is the most widely employed two-equation Reynolds Average Navier Stokes Equation Model. It is based on the solution of equations for the turbulent kinetic energy and the turbulent dissipation rate. The K.ϵ model can be derived from Incompressible Navier stokes equation. We can rewrite equation 6b as equation 15 below.

$$\rho\left(\frac{\partial v_i}{\partial t} + v_j\frac{\partial v_i}{\partial x_j}\right) = -\frac{\partial p}{\partial x_i} + \mu\nabla^2 v_i \tag{15}$$

Where $\boldsymbol{v(x,t)}$ represents the velocity vector field, ***p(x,t)*** is the pressure field, ϱ is the density, $\boldsymbol{\mu}$ is the dynamic viscosity and $\boldsymbol{\upsilon} = {}^{\boldsymbol{\mu}}/_{\boldsymbol{\rho}}$ is the kinematic viscosity.

We can rewrite equation 13b as shown below

$$\rho\frac{\partial\bar{v}_i}{\partial t} + \rho\bar{v}_j\frac{\partial\bar{v}_i}{\partial x_j} + \rho\frac{\partial}{\partial x_i}(\overline{v_i'v_j'}) = -\frac{\partial\bar{p}}{\partial x_i} + \frac{\partial\overline{\tau_{ij}}}{\partial x_j} \tag{16}$$

Multiply equation 15 by v_i and averaging it will give

$$\rho\overline{\frac{\partial v_i}{\partial t}v_i} + \rho\overline{v_j\frac{\partial v_i}{\partial x_j}v_i} = -\overline{\frac{\partial p}{\partial x_i}v_i} + \overline{\frac{\partial\tau_{ij}}{\partial x_j}v_i} \tag{17}$$

Multiplying equation 16 by v_i will give

$$\rho\frac{\partial\bar{v}_i}{\partial t}\bar{v}_i + \rho\bar{v}_j\frac{\partial\bar{v}_i}{\partial x_j}\bar{v}_i + \rho\frac{\partial}{\partial x_i}(\overline{v_i'v_j'})\bar{v}_i = -\frac{\partial\bar{p}}{\partial x_i}\bar{v}_i + \frac{\partial\overline{\tau_{ij}}}{\partial x_j}\bar{v}_i$$

or equivalently substituting equation 14 into the above equation we have

$$\rho\frac{\partial\bar{v}_i}{\partial t}\bar{v}_i + \rho\bar{v}_j\frac{\partial\bar{v}_i}{\partial x_j}\bar{v}_i + \rho\frac{\partial}{\partial x_i}\left(\overline{v_i'v_j'}\right)\bar{v}_i = -\frac{\partial\bar{p}}{\partial x_i}\bar{v}_i + \left(\frac{\partial\overline{\tau_{ij}}}{\partial x_j}\bar{v}_i + \frac{\partial T_{ij}}{\partial x_j}\bar{v}_i\right) \tag{18}$$

Subtracting equation 18 from equation 17

$$\rho\frac{\partial\bar{v}_i'}{\partial t}\bar{v}_i' + \rho\left(\overline{v_j\frac{\partial v_i}{\partial x_j}v_i} - \bar{v}_j\frac{\partial\bar{v}_i}{\partial x_j}\bar{v}_i\right) + \rho\frac{\partial}{\partial x_i}(\overline{v_i'v_j'})\bar{v}_i = -\frac{\partial\bar{p}'}{\partial x_i}\bar{v}_i' + \left(\frac{\partial\overline{\tau_{ij}'}}{\partial x_j}\bar{v}_i' + \frac{\partial T_{ij}}{\partial x_j}\bar{v}_i\right) \tag{19}$$

Where

$$\overline{\frac{\partial v_i}{\partial t}v_i} = \frac{\partial\bar{v}_i}{\partial t}\bar{v}_i + \overline{\frac{\partial v_i'}{\partial t}v_i'} \tag{20a}$$

$$\overline{\frac{\partial p}{\partial x_i}v_i} = \frac{\partial\bar{p}}{\partial x_i}\bar{v}_i + \overline{\frac{\partial p'}{\partial x_i}v_i'} \tag{20b}$$

$$\overline{\frac{\partial\tau_{ij}}{\partial x_j}v_i} = \frac{\partial\overline{\tau_{ij}}}{\partial x_j}\bar{v}_i + \overline{\frac{\partial v_i'}{\partial x_j}\tau_{ij}'} \tag{20c}$$

and

$$\overline{v_j \frac{\partial v_i}{\partial x_j} v_i} - \overline{v}_j \frac{\partial \overline{v}_i}{\partial x_j} \overline{v}_i = \overline{v_i' \frac{\partial v_i'}{\partial x_j}} \overline{v}_j + \overline{\frac{\partial v_i'}{\partial x_j} v_i' v_j'} + \overline{\frac{\partial v_i'}{\partial x_j} v_j'} \overline{v}_i + \overline{v_j' v_i'} \frac{\partial v_i'}{\partial x_j} \tag{20d}$$

By the average rules

Since $\overline{\tau_{ij}' v_i'}$ represents the viscous transfer of turbulent energy a very small quantity in contrast to the terms responsible for the turbulent transfer of turbulent energy in equation 19, it is neglected, thus equation 19 and the application of equation 20d becomes

$$\frac{\rho}{2}\left(\frac{\partial \overline{(v_i')^2}}{\partial t} + \frac{\partial \overline{(v_i')^2}}{\partial x_j} \overline{v}_j\right) = -\overline{\frac{\partial p'}{\partial x_i} v_i'} - \frac{\rho}{2} \frac{\partial}{\partial x_j} \overline{\left(v_i'^2 v_j'\right)} - \left(\frac{\partial v_i}{\partial x_j} \tau_{ij}' + \rho \overline{v_j' v_i'} \frac{\partial v_i}{\partial x_j}\right) \tag{21}$$

Summing over *i* 20 becomes an energy balance equation of turbulent flow:-

$$\rho\left(\frac{\partial k}{\partial t} + \sum_j \frac{\partial k}{\partial x_j} \overline{v}_j\right) = -\sum_j \frac{\partial}{\partial x_j}\left(\overline{p' v_j'} + \frac{\rho}{2} \sum_i \overline{v_i'^2 v_j'}\right) + \left(\overline{T_{ij}} \frac{\partial \overline{v}_i}{\partial x_j}\right) - \rho\epsilon \tag{22}$$

Where the turbulent kinetic energy is define as

$$k = \frac{1}{2} \overline{(v_i')^2} \tag{23}$$

And the rate of dissipation of the turbulent energy is

$$\epsilon = \frac{\partial v_i'}{\partial x_j} \tau_{ij}' = \frac{\upsilon}{2} \overline{\left(\frac{\partial v_i'}{\partial x_j} + \frac{\partial v_j'}{\partial x_i}\right)^2} \tag{24}$$

We can modify equation 22 using the Boussinesq assumption, to get the commonly use *k* model equation

$$\frac{\partial \rho k}{\partial t} + \frac{\partial}{\partial x_j}\left(\rho v_j k\right) = \frac{\partial}{\partial x_j}\left(\frac{\mu_t}{\sigma_k} \frac{\partial k}{\partial x_j}\right) + \tau_{ij} S_{ij} - \rho\epsilon \tag{25}$$

The Prandtl number σ_k connects the diffusivity of *k* to the eddy viscosity. A value of 1 is often used (Kestin, J. and Persen, L.N., 1962).

A model equation for rate of dissipation ϵ is derived by multiplying the *k* equation by ϵ/k and introducing model constants.

$$\frac{\partial\rho\epsilon}{\partial t}+\frac{\partial}{\partial x_j}\left(\rho v_j\epsilon\right)=\frac{\partial}{\partial x_j}\left(\frac{\mu_t}{\sigma_\epsilon}\frac{\partial\epsilon}{\partial x_j}\right)+C_{1\epsilon}\frac{\epsilon}{k}\tau_{ij}S_{ij}-C_{2\epsilon}\rho\frac{c^2}{k} \quad (26)$$

The Prandtl number σ_ϵ connects the diffusivity of ϵ to the eddy viscosity. Typically, a value of 1.30 is used. Typically values for the model constants $C_{1\varepsilon}$ and $C_{2\varepsilon}$ of 1.44 and 1.92 are used.

The terms on the right-hand side represent conservative diffusion, eddy-viscosity production and dissipation, respectively. The turbulent viscosity μ_t is calculated from:

$$\mu_t=C_\mu\frac{k^2}{\epsilon} \quad (27)$$

The Reynolds stresses are then calculated as follows:

$$T_{ij}=-\rho\overline{v_i'v_j'}=\mu_t\left(\frac{\partial v_i}{\partial x_j}+\frac{\partial v_j}{\partial x_i}\right)-\frac{2}{3}\rho k\delta_{ij} \quad (28)$$

The $\frac{2}{3}\rho k\delta_{ij}$ term ensures that the normal stresses sum to k.

Note that the k-ε model leads to all normal stresses being equal.

RESULTS AND DISCUSSION

The model is done for water flow in pipes with different diameter but the same pipe length. The Reynolds number considered for this turbulence modeling are 4000, 10,000 and 12,000 respectively. The turbulent flow pattern of the water flow is adequately considered and graphs were plotted in various layers along the pipe. The pipe is divided into segments for effective evaluation of turbulence in water across each pipe at the various Reynolds numbers.

Simulation 1: Turbulence modeling for water flow at Reynolds number of 4,000

This involves the prediction of turbulence in water flow along a pipe of length 1.2 m with diameter 0.16 m. The initial inlet velocity is around 0.025 m/s^2 and the Reynolds number simulated was 4,000 table 1 shows the Model constants and table 2 shows the boundary conditions.

Table 1: Model constants for simulation one

Name	Expressions / Value	Description
P	1000 [kg/m^3]	Density
N	0.001 [PaS]	Viscosity
v_o	0.025 [m/s^2]	Inlet Velocity
D	0.16 [m]	Diameter/ height
Re	$\varrho D v_o / v$ = 4000	Reynolds number

Table 2: Boundary conditions for simulation 1

Settings	Boundary 1	Boundary 2, 3	Boundary 4
Boundary type	Inlet	Wall	Outlet
Boundary conditions	Velocity	Logarithm wall function	Pressure
u_o	Vo = $0.025 m/s^2$		
v_o	0		
P_o			0

By using COMSOL Multiphysics software for the above simulation and modeling, the results obtained are shown in the figures below. Further investigation was carried out on the results obtain for velocity magnitude by dividing the pipe into layers of 0.025 m each as shown in figure 7. This is done so as to know the turbulent flow pattern at each of the layer of the water in the pipe and also to be able to understand the effect of the boundary layer on prediction of turbulence flow pattern in water.

Figure 1 is the initial geometry of the pipe before simulation. Figure 2, figure 3 and figure 4 show the turbulence flow pattern across the pipe. It is seen that the velocity magnitude which is a function of turbulence was maintained initially as the water was introduce into the pipe, the velocity magnitude was seen to be around 0.025 m/s^2which increase steadily across the pipe as the water moves towards the outlet to about 0.0275 m/s^2. We will appreciate the chaotic effect of turbulence more if we examine figure 4 which is the zoomed and enlarged image of the 2 dimensional flows; the chaotic effect of turbulence is seen clearly just like ripples.

The turbulent kinetic energy, k of the water flow in the pipe is seen to have a value that decreases across the pipe. Its highest value is around 2.344 X 10^{-6} m^2/s^2 and the lowest value at around 1.533 X 10^{-6} m^2/s^2. The turbulent kinetic energy is more at the inlet of the pipe and decreases towards the outlet of the pipe. The 2 dimensional image of turbulent kinetic energy is shown in figure 5.

The Turbulent dissipation rate, ε of the water flow in the pipe is seen to have a value that decreases across the pipe. Its highest value is around 1.362 X 10^{-6} $m^2/s^3$and the lowest value is around 2.033 X 10^{-7} m^2/s^3. The turbulent dissipation rate is more at the inlet of the pipe and decreases towards the outlet of the pipe. The 2 dimensional image of turbulent dissipation rate is shown in figure 6. This is the graphical representation of the data acquired during the modeling of each layers shown in figure 7. We can say that turbulence increase across the pipe as the velocity magnitude graph increases for layers 0.05 m, 0.075 m, 0.1 m, 0.125 m as shown in the graphs in figure 10, figure 11, figure 12 and figure 13 respectively on both sides of the pipe. The graph for layers 0.05 m show significant fluctuations which we can say is chaotic in nature and illustrate the increase of turbulent behaviour of water flow due to increase in the velocity magnitude, this layer is characterized with increase in velocity magnitude from around 0.025 m/s^2 to about 0.0265 m/s^2. Also, the graphs for layers 0.75 m, 0.1 m and 0.125 m show an increase in velocity magnitude from 0.025 m/s^2 to 0.0278 m/s^2, 0.025 m/s^2 to 0.0268 m/s^2 and 0.025 m/s^2 to 0.02518 m/s^2 respectively. From this observation, we can conclude that our water flow experience a high turbulent behaviour between layers within 0.05 m and 0.1 m, than any other layers in the pipe.

Along the walls of the pipe, turbulence decrease as velocity magnitude decreases, this is also true for layers that are next to the wall on both sides of the pipe. This decrease is because of boundary layer which is cause by the effect of viscosity. The velocity magnitude at the wall which is layers 0m and 0.16 m on both sides of the pipe decreases across the pipe from 0.025 m/s^2 to around 0.0215 m/s^2 as shown in figure 8 and figure 15. The velocity magnitude of the layer close to the wall, i.e. 0.025 m and 0.125 m on both sides of the pipe also decreases across the pipe length from 0.025 m/s^2 to around 0.0226 m/s^2 as shown in figure 9 and figure 14 respectively.

The reason for the change in the turbulent behavior across the various layers is due to Viscosity of the fluid. Viscosity is responsible for flow separation which causes major changes to the flow patterns as seen in the graphs.

Results for Simulation 1

Below are the results for the simulation of turbulence in water flow in pipe for Reynolds number 0f 4,000.

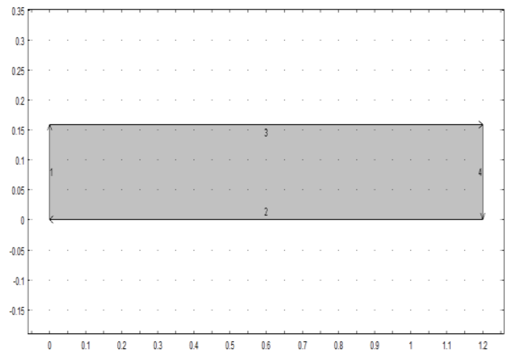

Figure 1: Initial Geometry of the pipe before simulation

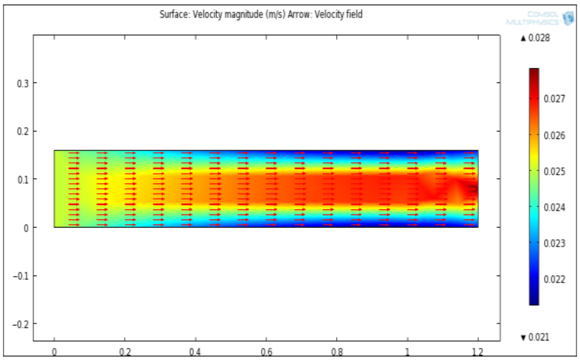

Figure 2: 2 Dimensional Image showing the direction of Turbulence flow in a pipe for water at Reynolds number 0f 4,000.

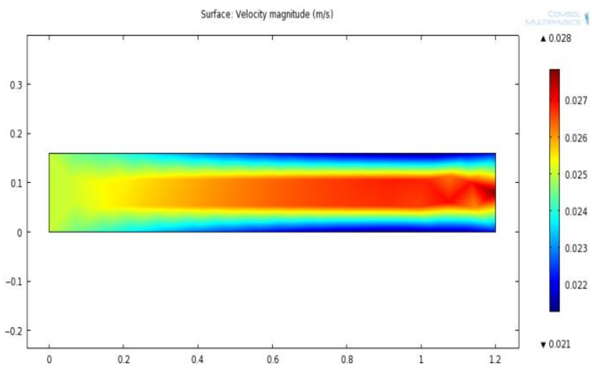

Figure 3: 2 Dimensional Image of Turbulent flow pattern in pipe for Water Flow at Reynolds Number of 4,000.

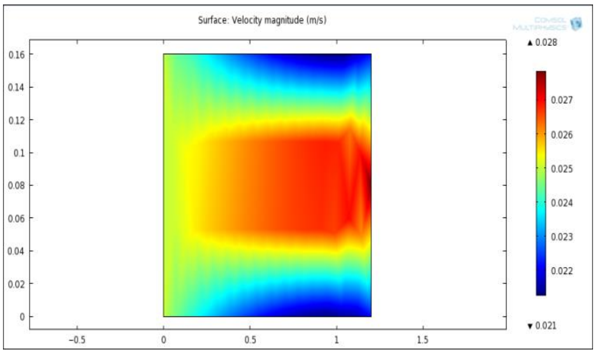

Figure 4: Zoomed 2 Dimensional Image of Turbulence flow pattern in pipe for Water at Reynolds number of 4000

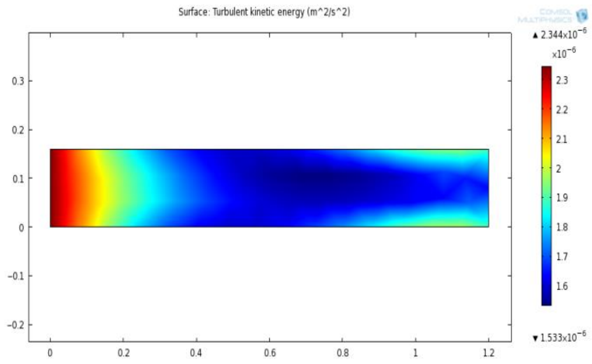

Figure 5: 2 Dimensional Image showing the Turbulence kinetic rate pattern in pipe for Water at Reynolds number of 4000.

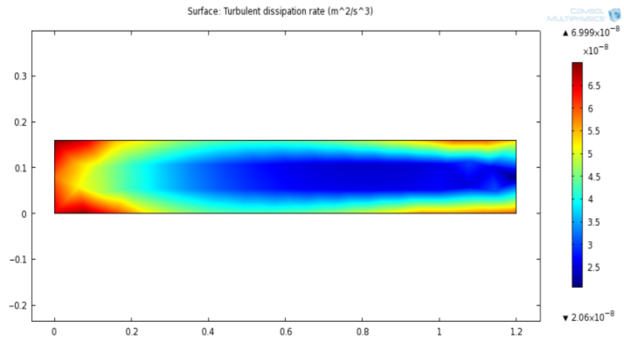

Figure 6: 2 Dimensional Image showing the Turbulence dissipation energy pattern in pipe for Water at Reynolds number of 4,000.

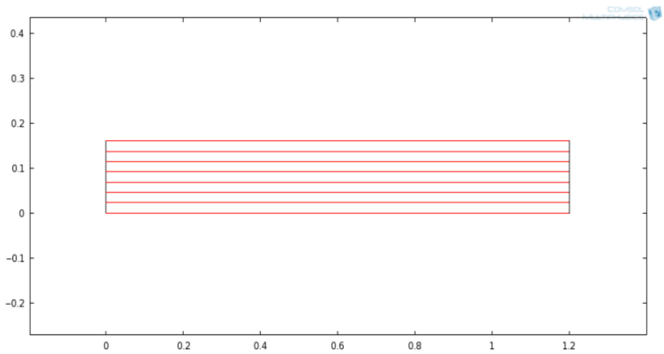

Figure 7: Divisions of the Pipe into Various Layers of 0.02 m Each for Turbulence Evaluation within the Pipe

Graphical representation of turbulence behaviors in water flow along the pipe.

The data acquire during the simulation and modeling of water flow at Reynolds number of 4000 along the pipe of length 1.2 m and diameter 0.16 m as shown in figure 6 above at various division and segment are use in plotting the graphs across various division of 0.0m, 0.025 m, 0.05 m, 0.075 m, 0.1m, 0.125 m, 0.15 m, 0.16 m respectively. The graphs were plotted using numerical values.

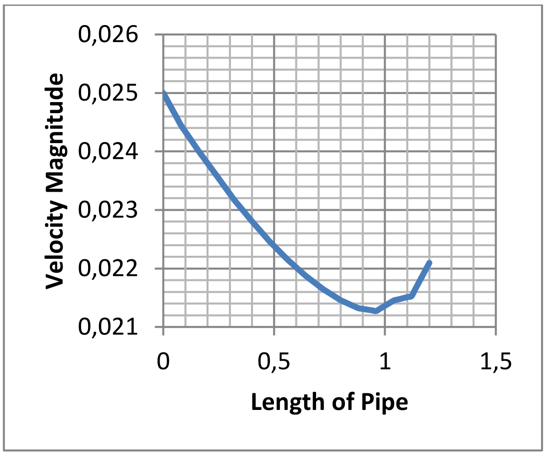

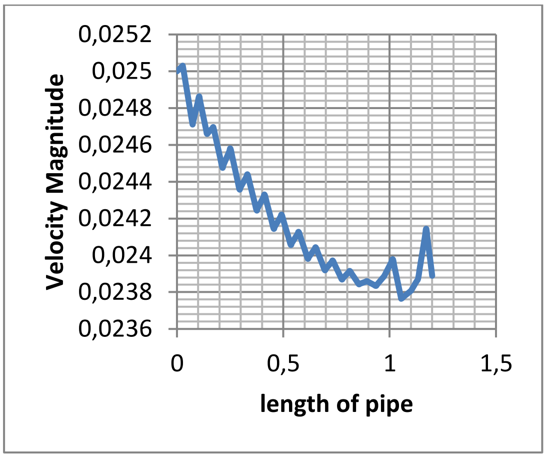

Figure 8: Turbulent flow pattern of water in a pipe along 0m at Reynolds number of 4000

Figure 9: Turbulent flow pattern of water in a pipe along 0.025m at Reynolds number of 4000

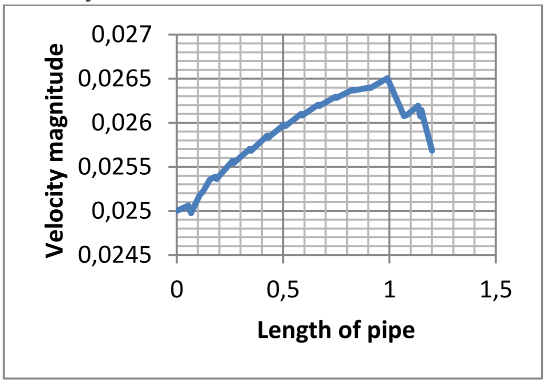

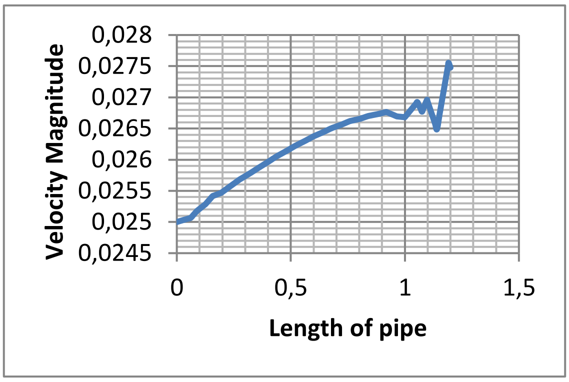

Figure 10: Turbulent flow pattern of water in a pipe along 0.05m at Reynolds number of 4000

Figure 11: Turbulent flow pattern of water in a pipe along 0.075m at Reynolds number of 4000

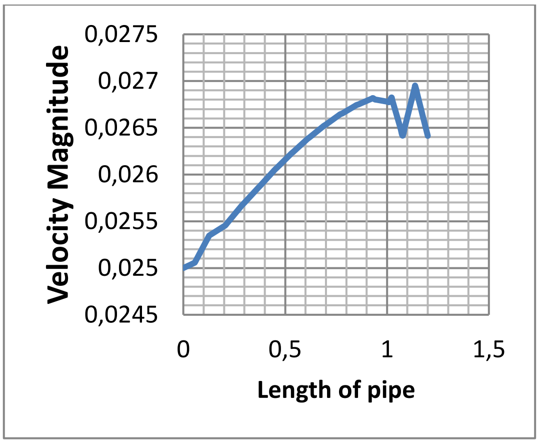

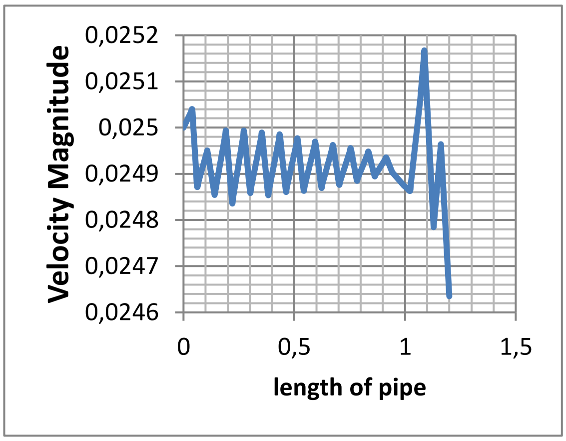

Figure 12: Turbulent flow pattern of water in a pipe along 0.1m at Reynolds number of 4000

Figure 13: Turbulent flow pattern of water in a pipe along 0.125m at Reynolds number of 4000

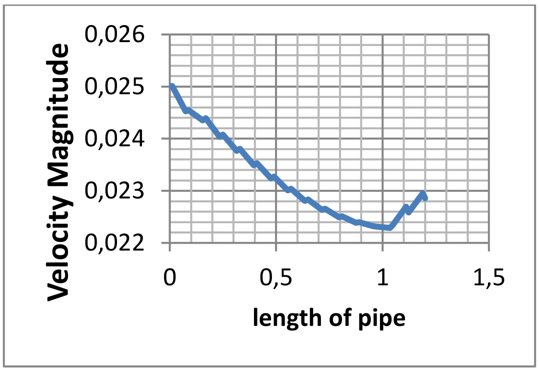

Figure 14: Turbulent flow pattern of water in a pipe along 0.15m at Reynolds number of 4000

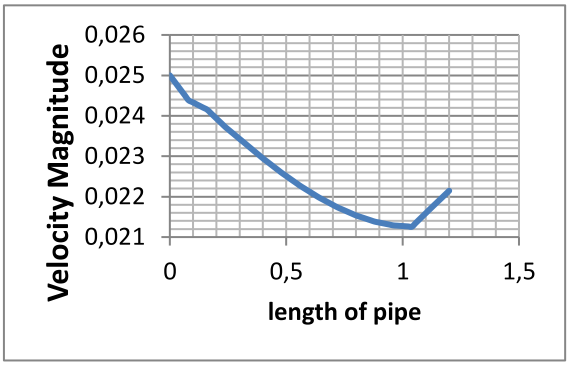

Figure 15: Turbulent flow pattern of water in a pipe along 0.16m at Reynolds number of 4000

Simulation 2: Turbulence modeling for water flow at Reynolds number of 10,000

This involves the prediction of turbulence in water flow along a pipe of length 1.2 m with diameter 0.15 m. The initial inlet velocity is around 0.0667 m/s^2 and the Reynolds number simulated was 10,000. Table 3 shows the Model constants and table 4 shows the boundary conditions.

Table 3: Model constants

Name	Expressions / Value	Description
P	1000 [kg/m^3]	Density
N	0.001 [PaS]	Viscosity
v_o	0.0667 [m/s^2]	Inlet Velocity
D	0.15 [m]	Diameter/ height
Re	$\varrho D v_o / v = 10000$	Reynolds number

Table 4: Boundary conditions for simulation 2

Settings	**Boundary 1**	**Boundary 2, 3**	**Boundary 4**
Boundary type	Inlet	Wall	Outlet
Boundary conditions	Velocity	Logarithm wall function	Pressure
u_o	Vo= 0.0667 m/s^2		
v_o	0		
P_o			0

By using COMSOL Multi physics software for the above simulation and modeling, the results obtained are shown in the figures below. Further investigation was carried out on the results obtain for velocity magnitude by dividing the pipe into layers of 0.025 m each as shown in Figure 14. This is done so as to know the turbulent flow pattern at each of the layer of the water in the pipe and also to be able to understand the effect of the boundary layer on prediction of turbulence flow pattern in water.

Figures: 17, 18 and 19 show the turbulence flow pattern across the pipe. It is seen that the velocity magnitude which is a function of turbulence was maintained initially as the water was introduce into the pipe, the velocity magnitude was seen to be around 0.0667 m/s which increase steadily across the pipe as the water moves towards the outlet. We appreciate the chaotic effect of turbulence more if we examine figure 19 which is the zoomed and enlarged image of the 2 dimensional flows, the chaotic effect of turbulence is seen clearly just like ripples.

The turbulent kinetic energy, k of the water flow in the pipe is seen to have a value that decreases across the pipe. Its highest value is around 1.668 X 10^{-5} m^2/s^2 and the lowest value at around 6.412 X 10^{-6} m^2/s^2. The turbulent kinetic energy is more at the inlet of the pipe and decreases towards the outlet of the pipe. The 2 dimensional image of turbulent kinetic energy is shown in figure 20.

The Turbulent dissipation rate, ε of the water flow in the pipe is seen to have a value that decreases across the pipe. Its highest value is around 1.362 X 10^{-6} $m^2/s^3$and the lowest value at around 2.033 X 10^{-7} m^2/s^3. The turbulent dissipation rate is more at the inlet of the pipe and decreases towards the outlet of the pipe. The 2 dimensional image of turbulent dissipation rate is shown in figure 22, represents the data acquired during the modeling of each layer, as also depicted in Figure 22.

We can say that turbulence increase across the pipe as the velocity magnitude graph increases for layers 0.05 m, 0.075 m, 0.1 m as shown in three graphs, figures: 25, 26 and 27 respectively on both sides of the pipe. The graph for layers 0.05 m show significant fluctuations which we can say is chaotic in nature and illustrate the increase of turbulent behaviour of water flow due to increase in the velocity magnitude, this layer is characterized with increase in velocity magnitude from around 0.06666 m/s^2 to about 0.0683 m/s^2. Also, the graphs for layers 0.75 m and 0.1 m show an increase in velocity magnitude. From this observation, we can conclude that our water flow experience a high turbulent behaviour between layers within 0.05 m and 0.2 m, than any other layers in the pipe.

Along the walls of the pipe, turbulence decrease as velocity magnitude decreases, this is also true for layers that are next to the wall on both sides of the pipe. This decrease is because of boundary layer which is cause by the effect of viscosity. The velocity magnitude of the wall which is layers 0 m and 0.15 m on both sides of the pipe decreases across the pipe from 0.0667 m/s^2 to around 0.0637 m/s^2 as shown in figures 23 and 29 respectively. The velocity magnitude of the layer close to the wall, i.e. 0.025 m and 0.125 m on both sides of the pipe also decreases across the pipe length from 0.0667 m/s^2 to around 0.06584 m/s^2 as shown in figures 24 and 28 respectively.

The reason for the change in the turbulent behavior across the various layers is due to Viscosity of the fluid. Viscosity is responsible for flow separation which causes major changes to the flow patterns as seen in the graphs.

Results for Simulation 2

Below are the results for the simulation of turbulence in water flow in pipe for Reynolds number 0f 10000

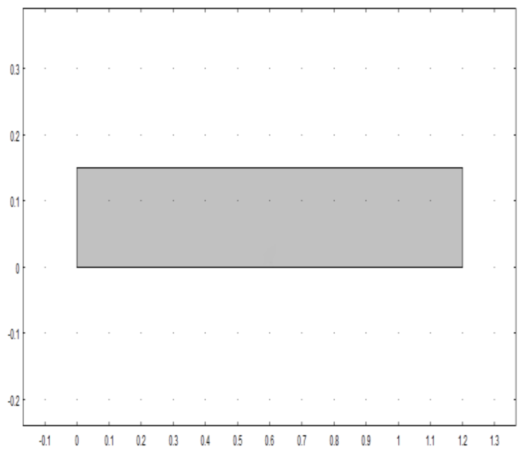

Figure 16: Initial geometry of the pipe before simulation

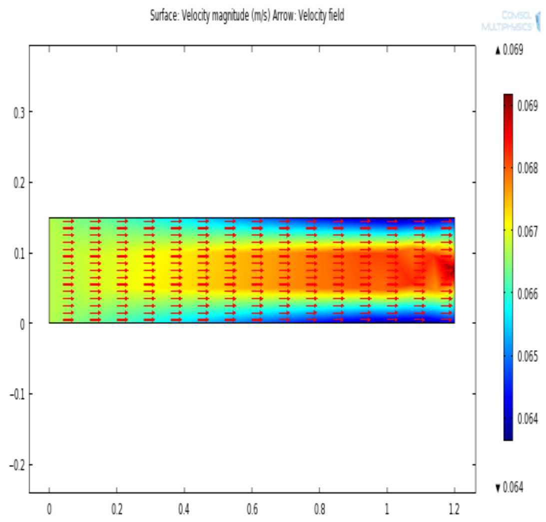

Figure 17: 2 Dimensional Image showing the direction of Turbulence flow in a pipe

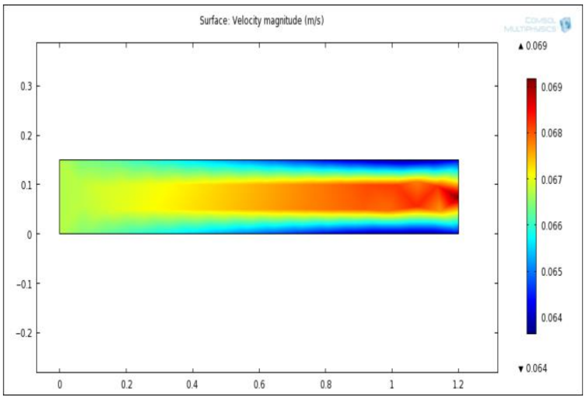

Figure 18: 2 Dimensional Image of Turbulent flow pattern in a Pipe pattern for water at Reynolds Number of 10,000.

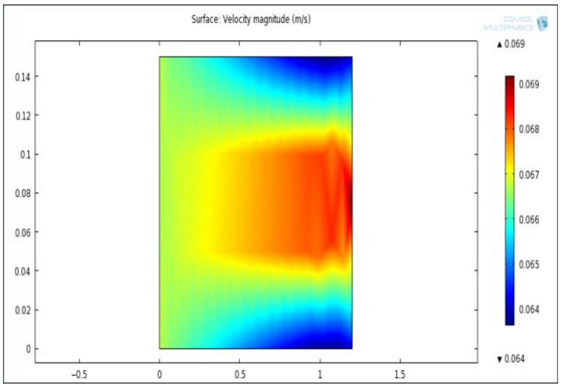

Figure 19: Zoomed 2 Dimensional Image of Turbulence flow in a Pipe for water at Reynolds number of 10000.

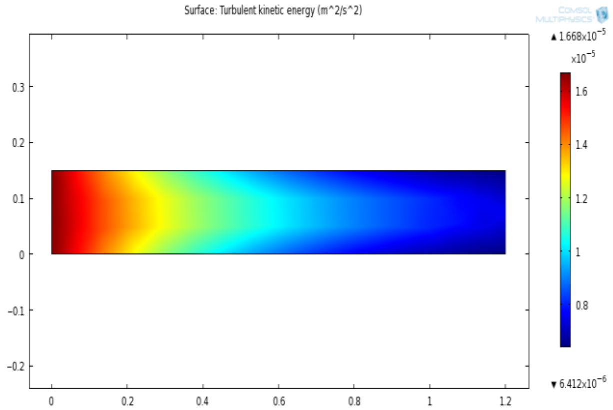

Figure 20: 2 Dimensional Image showing the Turbulence kinetic energy pattern in pipe for Water at Reynolds number of 10,000.

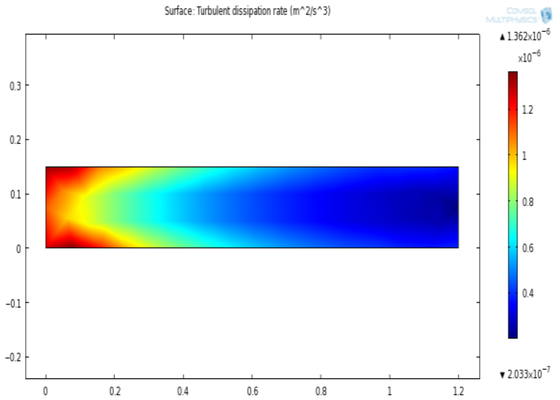

Figure 21: 2 Dimensional Image showing the Turbulence dissipation rate pattern in pipe for Water at Reynolds number of 10,000.

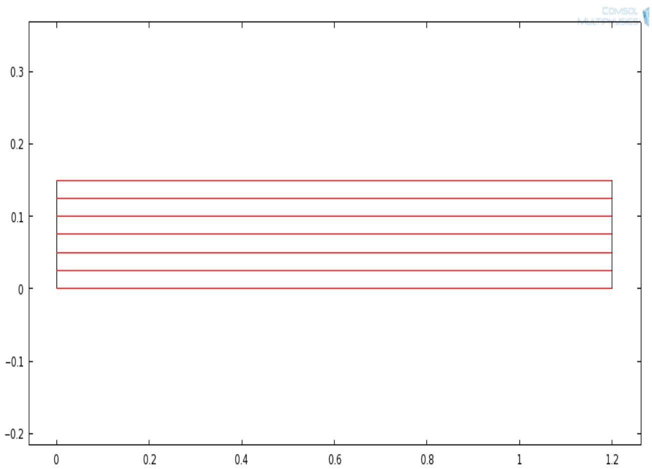

Figure 22: Divisions of the Pipe into Various Layers of 0.025m Each for Turbulence Evaluation within the Pipe.

Graphical Representation of Turbulence Behaviors in Water Flow Along the Pipe

The data acquire during the simulation and modeling of water flow at Reynolds number of 10,000 along the pipe of length 1.2 m and diameter 0.15 m as shown in figure 22 above at various division and segment are use in plotting the graphs across various division of 0.0 m, 0.025 m, 0.05 m, 0.075 m, 0.1 m, 0.125 m, 0.15 m, 0.15 m, respectively. The graphs were plotted using numerical values.

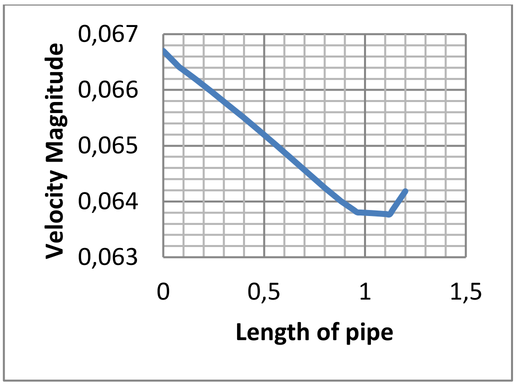

Figure 23: Turbulent flow pattern of water in a pipe along 0.0m at Reynolds number of 10000

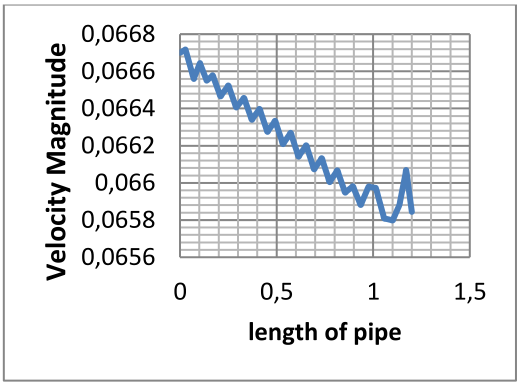

Figure 24: Turbulent flow pattern of water in a pipe along 0.025m at Reynolds number of 10000

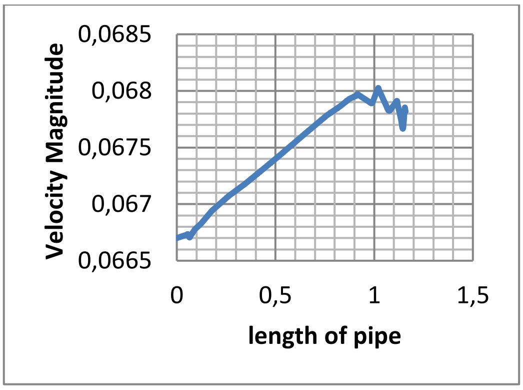

Figure 25: Turbulent flow pattern of water in a pipe along 0.05m at Reynolds number of 10000

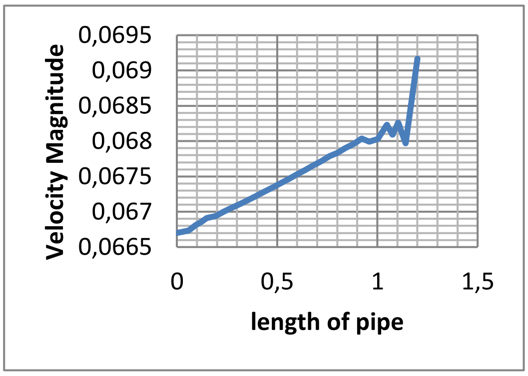

Figure 26: Turbulent flow pattern of water in a pipe along 0.075m at Reynolds number of 10000

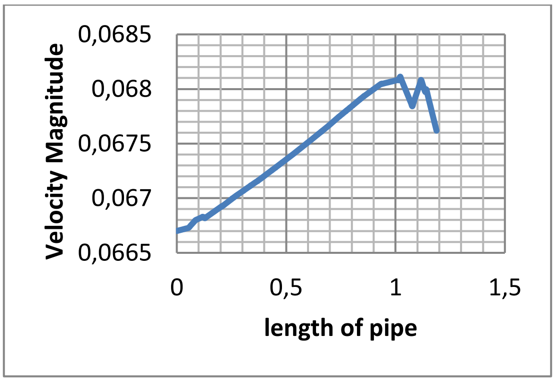

Figure 27: Turbulent flow pattern of water in a pipe along 0.1m at Reynolds number of 10000

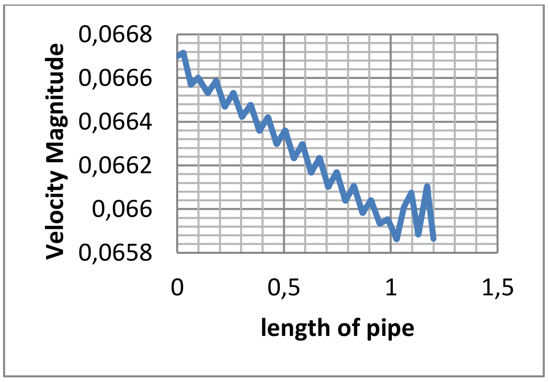

Figure 28: Turbulent flow pattern of water in a pipe along 0.125m at Reynolds number of 10000

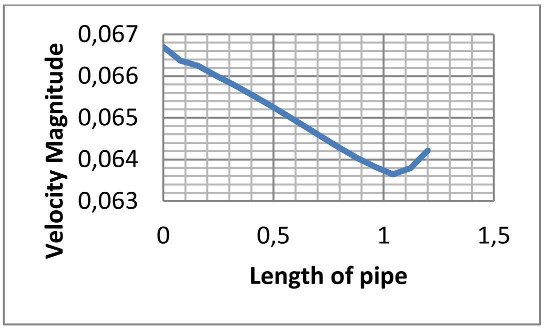

Figure 29: Turbulent flow pattern of water in a pipe along 0.15m at Reynolds number of 10000

Discussion

The turbulent nature of water in pipe as seen in the simulation is seen to vary with different Reynolds number, velocity and diameter. When there is closeness in the diameter of the pipes use in modeling the water flow in the simulation, there will be a kind of similarity in 2 dimensional image of turbulent flow pattern in pipe for water. The other significant phenomena worthy of note is the viscous effect of the various layer of the fluid considered and the similarity in the graphs of layers that are on exactly the same point on each side of the pipe as in figure 8 and figure 15.

The velocity profile in the entire pipe shows that the fluid at the center of the stream moves more quickly than the fluid towards the edge of the stream. Therefore, friction will occur between layers within the fluid.

Fluids with a high viscosity will flow more slowly and will generally not support eddy currents and therefore the internal roughness of the pipe will have no effect on the frictional resistance. In large diameter pipes the overall effect of the eddy currents is less significant. In small diameter pipes the internal roughness can have a major influence on the friction factor.

CONCLUSION

The model performs particularly well in confined flows where the Reynolds shear stresses are most important. This includes a wide range of flows with industrial engineering applications, which explains its popularity. The standard k-ϵ model shows only moderate agreement in unconfined flows which is an example of complex flow. Turbulence flow pattern in pipe for water can be said to be dependent on the Reynolds number, inlet velocity, diameter and length of pipe and the type of pipe.

Recommendation

The velocity profile or magnitude of water flow in a pipe is always affected by factors which include the viscosity, velocity, pressure and temperature, hence, simulation must be carried out under ideal condition because any change in one or two of this factors, may lead to a total change in the simulation result. It is advisable to go for Large Eddy simulation which will give a precise and near to experimental value result for the modeling of complex flows. When using COMSOL Multiphysics software for turbulence modeling, the various boundary conditions involve should be consider because they have a lot to do with the outcome of the simulation.

Funding

There is no funding for this work

Competing Interests

There is no competing interest that are directly or indirectly related to the work

REFERENCES

Acheson, D. (1990). Elementary Fluid Dynamics, Oxford Applied Mathematics and Computing Science Series. *Oxford University Press.*

Batchelor, G. K. (1967). An Introduction to Fluid Dynamics. *Cambridge University Press.*

Boussinesq, J. (1897). Theorie de l'ecoulement Turbillonnant et Tumultueux des Liquides Dans les lits Rectilignes a Grande Section. *Paris: Gaulthier-Villars*

Geankoplis, C. J. (2003). Transport Processes and Separation Process Principles. *Prentice Hall Professional Technical Reference.*

Kestin, J. and Persen, L.N. (1962). The transfer of heat across a turbulent boundary layer at very high prandtl numbers. *Int. J. Heat Mass Transfer 5, 355–371.*

Launder, B. E. (1991, March 18-21). "An Introduction to the Modeling of Turbulence,". *VKI Lecture Series , pp. 1- end.*

Lerner, R., & Trigg, G. (1991). Encyclopaedia of Physics (2nd Edition). *VHC publishers.*

Lesieur, M. (1990). Turbulence in Fluids. *4th edition. Netherland: Springer.*

Potter, M & Wiggert, D. (2008). Fluid mechanics (Schuam's Series*). McGraw-Hill(USA): Schuam Outlines.*

Lushchik, V. G., Makarova, M. S, and Reshmin, A. I (2023). Numerical Simulation of Turbulent Flow Control at Pipe Inlet to Advance Flow Relaminarization.*Fluid Dynamics, 2023, Vol. 58, No. 1, pp. 58–74*.

Zaiko, Y. S., Reshmin, A. I., Teplovodskii, S. K. and Chicherina, A. D. (2018). Investigation of Submerged jets with an extended initial laminar region. *Fluid Dynamics, volume 53, Page 95 – 104*.

Zayko, J., Teplovodskii, S., Chicherina, A., Vedeneev, V., and Reshmin, A. (2018). Formation of free round jets with long laminar regions at large Reynolds numbers, Phys *Fluids, volume 30, no. 4 P043603*.

Scarselli, D., Kuhnen, J., and Hof, B. (2019). Relaminarising pipe flow by wall movement, *J. Fluid Mech., 2019, vol. 867, pp. 934–948*.